Check for updates

Investigating the performance of agricultural wastes and their ashes in removing phenol from leachate in a fixed-bed column

Seyed Omid Ahmadinejad, Seyed Taghi Omid Naeeni, Zahra Akbari and Sara Nazif

ABSTRACT

One of the major pollutants in leachate is phenol. Due to safety and environmental problems, removal of phenol from leachate is essential. Most of the adsorption studies have been conducted in batch systems. Practically, large-scale adsorption is carried out in continuous systems. In this research, the adsorption method has been used for phenol removal from leachate by using walnut shell activated carbon (WSA) and coconut shell activated carbon (CSA) as adsorbents in a fixed-bed column. The effect of adsorbent bed depth, influent phenol concentration and type of adsorbent on adsorption was explored. By increasing the depth of the adsorbent bed in the column, phenol removal efficiency and saturation time increase significantly. Also, by increasing the influent concentration, saturation time of the column decreases. To predict the column performance and describe the breakthrough curve, three kinetic models of Yon-Nelson, Adams-Bohart and Thomas were applied. The results of the experiments indicate that there is a good match between the results of the experiment and the predicted results of the models.

Key words | activated carbon, adsorption, continuous flow, leachate, phenol

Seyed Omid Ahmadinejad (corresponding author)
Seyed Taghi Omid Naeeni
Zahra Akbari
Sara Nazif
School of Civil Engineering, College of Engineering, University of Tehran,
Tehran,
Iran
E-mail: *omidahmadinejad@ut.ac.ir*

HIGHLIGHTS

- Agricultural products were used as adsorbents.
- Adsorption was the method used for removal of phenol from leachate.
- The effect of influent concentration, type of adsorbent and adsorbent bed depth on phenol adsorption was explored.
- Phenol was removed efficiently in a fixed-bed column.
- To predict the column performance and describe the breakthrough curve, three kinetic models were applied.

INTRODUCTION

The rising standard of living in societies and the continuous growth of industry and trade in many countries have gone along with rapid increment in the production of industrial and municipal solid waste (MSW). The generation of MSW is increasing per capita and in total (Warah 2001). For instance, in 2012, solid waste production in all cities of the world was 1.3 billion tonnes which was 1.2 kg per capita per day. Estimates indicate that these numbers will be 2.2 billion tonnes per year and 1.42 kg per capita per day by 2025 (Show *et al.* 2019). Different methods have been used for the disposal of municipal solid waste (MSW) and the most commonly employed method is sanitary landfilling. Disposal of MSW in landfills has numerous environmental problems. Combination of the deteriorated organic compounds of the waste in the landfill and infiltrated rainwater makes a liquid known as 'leachate' (Rodríguez *et al.* 2004). Threats of leachate to society are increasing due to the possibility of polluting groundwater and affecting soil fertility negatively.

doi: 10.2166/wst.2020.274

Downloaded from http://iwaponline.com/wst/article-pdf/81/10/2109/716478/wst081102109.pdf
by guest

There is a wide range of organic matter in leachate such as humic substances, phenolic compounds, ammonia nitrogen, chlorinated organic and toxic metals (Sanjay *et al.* 2013). The United States Environmental Protection Agency (EPA) has declared that phenol is one of the main pollutants in water. Serious harmful effects caused by phenols in humans are anorexia, nausea, headaches, a problem swallowing, and fainting (Pajooheshfar & Saeedi 2009). In addition to municipal waste, industrial waste leachate also contains phenol. Phenol is present in industrial leachate such as petrochemical complexes (2.8–1,220 mg l^{-1}), coal production processes (9–6,800 mg l^{-1}) and refineries (6–500 mg l^{-1}). Other industries that contain 0.1–1,600 mg l^{-1} of phenol are paper, pharmaceutical, wood, paint and plastic industries (Mohammadi *et al.* 2015). Because of phenol toxicity, the phenol level in the environment has been limited. For instance, 0.001 mg l^{-1} has been recommended by the World Health Organization (WHO) as the allowable concentration of phenol in drinking water (Srivastava *et al.* 2006).

Numerous methods for removing phenolic compounds from wastewater and water have been used. These include techniques like chemical oxidation, adsorption, extraction and biodegradation (Mohammadi *et al.* 2015). To remove phenols from aqueous solution, adsorption is a powerful technique and activated carbons are popular adsorbents to use in adsorption process (Mahvi *et al.* 2004). Activated carbons have high mechanical strength, high specific surface area and sufficient pore size distribution that these advantages make them good adsorbents for organic pollutants (Goud *et al.* 2005). Activated carbon preparation and regeneration by desorbing adsorbed contaminants via techniques like thermal reactivation (Bagreev *et al.* 2001), chemical and solvent regeneration (Martin & Ng 1987), microbial regeneration (Aizpuru *et al.* 2003), electrochemical regeneration (Narbaitz & Karimi-Jashni 2009), ultrasonic regeneration (Lim & Okada 2005) and wet air oxidation (Shende & Mahajani 2002) are expensive and that is the reason why there has always been a search for inexpensive adsorbents, particularly those which are made out of agricultural products since they are available in large quantities and in terms of costs are also affordable (Volesky 2003).

Rengaraj *et al.* (2002) carried out adsorption studies to remove phenol from water and wastewater by activated palm seed coat carbon (PSCC). Their study expressed that commercial activated carbon is less effective than PSCC. Activated carbons produced by nutshells have also been used for phenol removal from aqueous solutions and effects of flow rate, adsorbent particle size and influent phenol concentration on phenol adsorption were examined (Goud *et al.* 2005; Pajooheshfar & Saeedi 2009). Mahvi *et al.* (2004) conducted a study of phenol adsorption by rice husk and its ash from aqueous solutions as a function of phenol concentration, pH, contact time and adsorbent dose through batch experiments. It was shown in their study that rice husk ash is an efficient adsorbent to remove phenol from water and wastewater. The researchers reported that there is a good potential for the adsorption of phenol in bagasse fly ash (Srivastava *et al.* 1995; Gupta *et al.* 1998). Published reports revealed that there are other low cost adsorbents such as straw (Streat *et al.* 1995), waste activated sludge (Aksu & Yener 2001) and fertilizer waste (Srivastava *et al.* 1997) that have a good performance in removing phenol from water and wastewater. Wenzel *et al.* (1999) applied UV/O_3 as an advanced oxidation process for landfill leachate treatment. Their study investigated degradation of organic compounds and it resulted in a phenol removal rate of 100%. Orupold *et al.* (2000) explored the possibility of biological lagooning to remove phenol from leachate. A removal of 80–88% of phenol was achieved. Their study also indicated that there is no need to adjust pH for the biological treatment of leachate of high pH. Aziz *et al.* (2012) used sequencing batch reactors (SBRs), powdered activated carbon (PAC-SBR) and non-powdered activated carbon (NPAC-SBR), for removal of phenol from raw leachates at two landfill sites. Phenol removal efficiencies at one of the sites in PAC-SBRs and NPAC-SBRs were 55% and 25%, respectively, while those values at the other site were 97.75% and 94.81%, respectively. It was concluded that PAC enhanced phenol removal rates. Dan *et al.* (2017) used constructed wetlands for phenol removal from synthetic leachate and 88–100% of removal rate was obtained. In the study, batch adsorption method and subsequent biodegradation were applied as the initial and main removal process, respectively.

Despite recent research and studies in the field of leachate, leachate is still a problem for the environment protection. Some countries have not yet realized the importance of leachate as a liquid that could harm the environment. Also, in those countries in which leachate treatment has developed, many of the treatment methods have low efficiency. In particular, due to the greater use of other leachate treatment methods than adsorption, gaps can be noticed in phenol removal from leachate via adsorption, and also most of the adsorption studies in water, wastewater and leachate treatment have been conducted in batch systems but practically, large-scale adsorption is carried out in continuous systems. Furthermore, Iran has a rich agriculture that made objectives for this study to

Downloaded from http://iwaponline.com/wst/article-pdf/81/10/2109/716478/wst081102109.pdf
by guest

investigate using agricultural wastes as sources to prepare the adsorbents used in the adsorption process in a continuous system. The present work studies the possibility of using a fixed-bed column of walnut shell activated carbon (WSA), coconut shell activated carbon (CSA) and coal activated carbon (CAC) as adsorbents for the removal of phenol from leachate. WSA and CSA were used due to their low cost and because they have not been used in a fixed-bed column for phenol removal from leachate in previous studies. We have used CAC as the standard adsorbent to evaluate the adsorptive attributes of WSA and CSA. The effect of several parameters including adsorbent bed depth, influent phenol concentration and type of adsorbent on adsorption was investigated. The Yoon-Nelson, Adams-Bohart and Thomas models were applied to predict the performance of adsorbents.

MATERIALS AND METHODS

In this section, mathematical description, adsorbents, adsorbate, Fourier transform infrared (FTIR) spectroscopy and column experiments are presented.

Mathematical description

Breakthrough curve is the profile that describes the adsorption behavior of a fixed-bed column. Breakthrough curve characteristics are dependent on the column capacity with respect to the type of adsorbent, adsorbent bed depth and feed concentration. The column performance in the breakthrough curve is expressed in term of the ratio of effluent phenol concentration to influent phenol concentration (C_t/C_0) as a function of time or volume of effluent for a given bed height. Effluent volume (V_{eff}) can be calculated from Equation (1).

$$V_{eff} = Qt_{total} \tag{1}$$

where t_{total} and Q are the total flow time (min) and volumetric flow rate (ml min^{-1}) (Aksu & Gönen 2004).

Design of an adsorption column needs prediction of the breakthrough curve. In this study, kinetic models were applied to express the column's dynamic process.

Thomas model

The Thomas model is one of the most basic and trusted methods for describing the performance of the fixed-bed columns. This model has the following linearized form:

$$\ln\left(\frac{C_0}{C_t} - 1\right) = \frac{k_{Th}q_0X}{Q} - k_{Th}C_0t \tag{2}$$

where C_0 and C_t are the influent and effluent phenol concentrations (mg l^{-1}); k_{Th} is the Thomas rate constant (ml min^{-1}mg^{-1}); q_0 is the maximum solid-phase concentration of the solute (mg g^{-1}) and X is the mass of the adsorbent (g), respectively. The parameters of k_{Th} and q_0 can be determined using a plot of $\ln\left(\frac{C_0}{C_t} - 1\right)$ against t at a given flow rate (Rao & Viraraghavan 2002).

Yoon-Nelson model

The model was developed by Yoon and Nelson which focused on the adsorption associated with vapors and also gases in activated charcoal. The equation of this model is presented as follows:

$$\ln\left(\frac{C_t}{C_0 - C_t}\right) = k_{YN}t - \tau k_{YN} \tag{3}$$

where C_0 and C_t are the influent and effluent phenol concentrations (mg l^{-1}); k_{YN} is the rate constant (min^{-1}); τ is the time required for 50% adsorbate breakthrough (min) and t is the breakthrough time (min). The parameters of k_{YN} and τ can be determined using a plot of $\ln\left(\frac{C_t}{C_0 - C_t}\right)$ against t according to Equation (3) (Tsai 1999).

Adams-Bohart model

In this model, it is assumed that the adsorption rate is affected by the concentration of the adsorbate and the residual capacity of the adsorbent. This model has the following linearized form:

$$\ln\frac{C_t}{C_0} = k_{AB}C_0t - k_{AB}N_0\frac{Z}{U_0} \tag{4}$$

where C_0 and C_t are the influent and effluent phenol concentrations (mg l^{-1}); k_{AB} is the kinetic constant (l min^{-1} mg^{-1}); N_0 is the saturation concentration (mg l^{-1}); U_0 is the superficial velocity (cm min^{-1}) and Z is the column depth (cm). These values can be obtained by using a plot of $\ln\frac{C_t}{C_0}$ against t at a specific flow rate and bed height (Aksu & Gönen 2004).

Downloaded from http://iwaponline.com/wst/article-pdf/81/10/2109/716478/wst081102109.pdf
by guest

Adsorbents

The WSA, CSA and CAC were procured from local suppliers. Table 1 presents the adsorbents characteristics.

Adsorbate

Phenol (C_6H_6O), supplied by Merck, was used to prepare synthetic solutions. The range of influent phenol concentrations was between 20 and 100 (mg l^{-1}) to appropriately simulate phenol concentration in leachate

Fourier transform infrared spectroscopy

To identify functional groups of the adsorbents before and after the adsorption, FTIR spectroscopy was used. We obtained FTIR spectra of the samples by using a Bruker Tensor 27 FTIR spectrometer at wavenumber of 400 to 4,000 cm^{-1}.

Table 1 | Adsorbents characteristics

Characteristics	WSA	CSA	CAC
Total surface area (B.E.T.) (m^2g^{-1})	1,000	1,150	1,150
Ash content (%)	8	0.5	12
Apparent density (kgm^{-3})	410	510	470
pH	Alkaline	Neutral	Alkaline

Column experiments

To perform column experiments, a plastic fixed-bed column of 2.6 cm internal diameter and 20 cm height has been used. A layer of glass wool was placed at the bottom of the column to hold the absorbent and prevent it from depositing below the bed. There was another layer of glass wool above the bed to prevent it from floating and washing. The experimental model also included two containers. The second container, with a capacity of 10 liters, was used for phenol solution storing and there was a floater inside it for fixing the flow rate. The first container, with a capacity of 20 liters, was located above the second container so it would feed the second container if needed. At the bottom of the first container there was an inlet hose connected to the floater inside the second container. The second container had a flow regulating valve at the bottom where the outlet hose was connected to the bottom of the column. For all experiments, an upward flow of 40 ml min^{-1} constant rate was considered and every 30 minutes, frequent checks were made to correct any changes in the flow rate. Finally, for measuring the residual phenol concentration, effluent samples of 25 ml volume were collected at intervals of 60 minutes and analyzed using a spectrophotometer (PhotoLab 6600 UV/VIS). Figure 1 shows the schematic diagram of the experimental model.

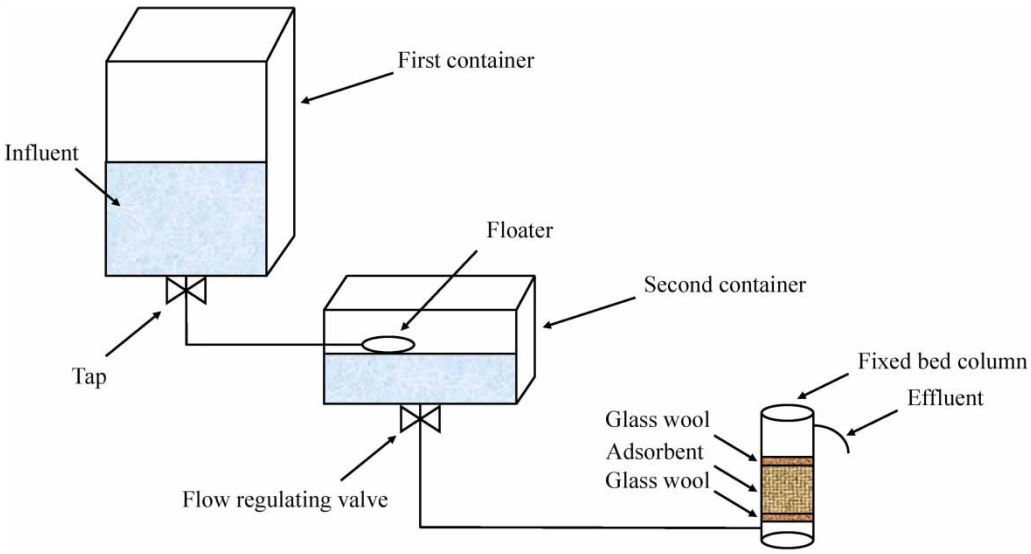

Figure 1 | Schematic diagram of the experimental model.

Downloaded from http://iwaponline.com/wst/article-pdf/81/10/2109/716478/wst081102109.pdf
by guest

RESULTS AND DISCUSSION

Investigating functional groups in adsorbents

All adsorbents were sampled before and after phenol adsorption and they were analysed by using an FTIR spectroscope. No peak shifts in the adsorbent indicate physical adsorption (Simaratanamongkol & Thiravetyan 2010). As shown in Figures 2–4 and Table 2, peak elimination and also changes in the peak of the CAC and WSA functional groups after adsorption illustrate that chemical adsorption has occurred. But in the case of CSA, no significant changes are observed in peaks before and after adsorption so it can be concluded that physical adsorption has happened. FTIR images show that the band at 2,911–2,922 cm^{-1}, which indicates the C-H stretching vibration has been weakened and could indicate a hydrogen element that has been partially removed during the adsorption process. The band at 3,400–3,500 cm^{-1} in all samples is related to the O-H stretching vibration of adsorbed water and hydroxyl groups. This band indicates the presence of strong hydrogen bonds such as phenol, alcohol and carboxylic acid (Yakout & Sharaf El-Deen 2016).

Table 2 shows the wavenumber of functional groups in the spectrum before and after adsorption for adsorbents.

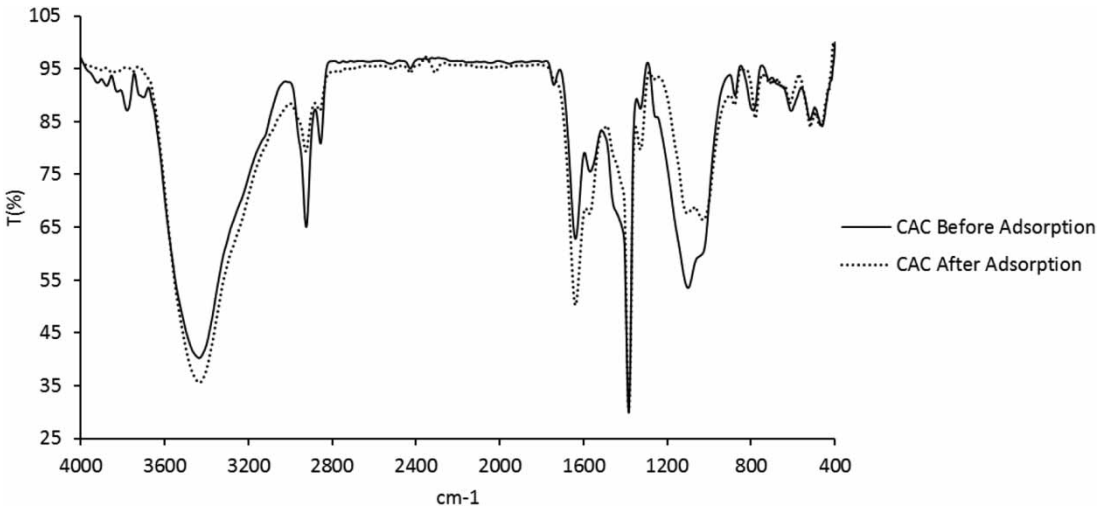

Figure 2 | FTIR spectrum of CAC before and after adsorption.

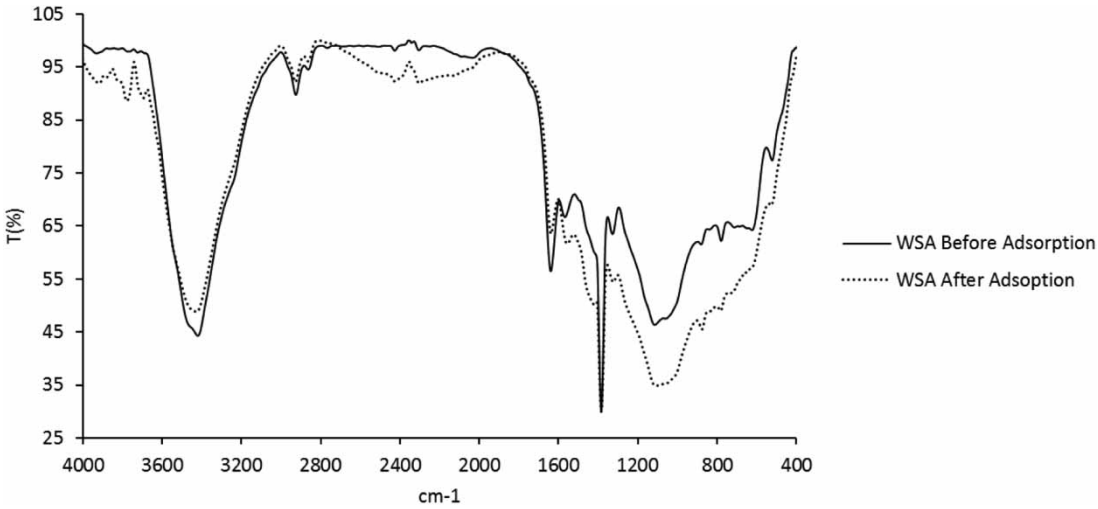

Figure 3 | FTIR spectrum of WSA before and after adsorption.

Downloaded from http://iwaponline.com/wst/article-pdf/81/10/2109/716478/wst081102109.pdf
by guest

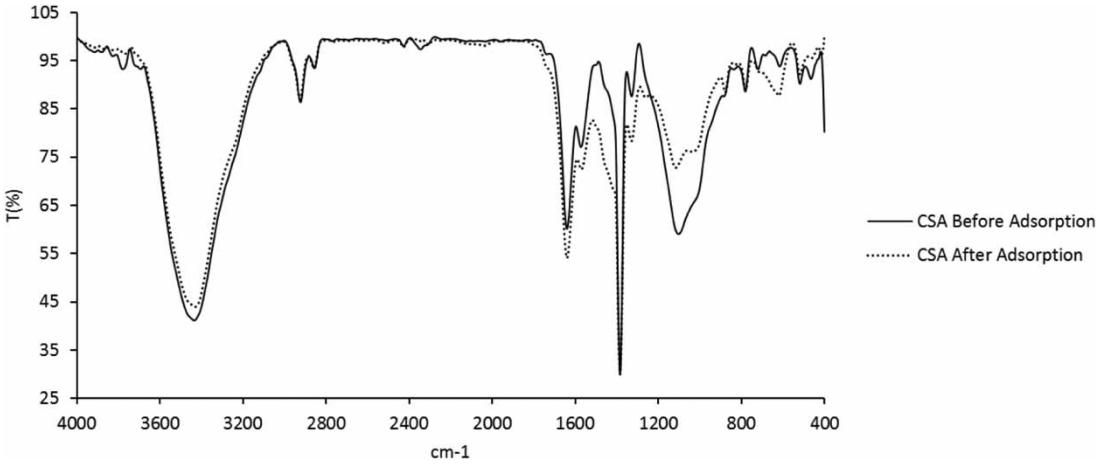

Figure 4 | FTIR spectrum of CSA before and after adsorption.

Table 2 | Wavenumber of functional groups in the spectrum

Type of the adsorbent	wavenumber	Functional group
WSA-before adsorption	3,419	C(=O)OH
	2,923	O-H
	2,855	C-H
	1,638	C = O
WSA-after adsorption	3,426	C(=O)OH
	2,927	O-H
	–	C-H
	1,638	C = O
CSA-before adsorption	3,434	C(=O)OH
	2,923	O-H
	–	C-H
	1,639	C = O
CSA-after adsorption	3,430	C(=O)OH
	2,925	O-H
	–	C-H
	1,638	C = O

Effect of bed depth

Figures 5–10 show the breakthrough curves obtained by changing the bed depth of adsorbents. It can be seen from them that the higher the depth of the bed, the more time the phenol has to contact with the adsorbents, which leads to increase in the phenol removal efficiency in the column. This finding appears in the lower value of C_t/C_0 in 8 cm of adsorbents in comparison to 4 cm of them at the same time. As the bed depth increases, adsorbent surface area increases and therefore saturation time increases significantly. Considering Figures 9 and 10 as examples, with 100 mg l^{-1} of phenol concentration, saturation time for 4 cm of WSA and CSA is 300 and 240 minutes, respectively, while this value for 8 cm of the adsorbents is 600 and 420 minutes, respectively. The volumes of solutions treated by the column also increases by increase in the saturation

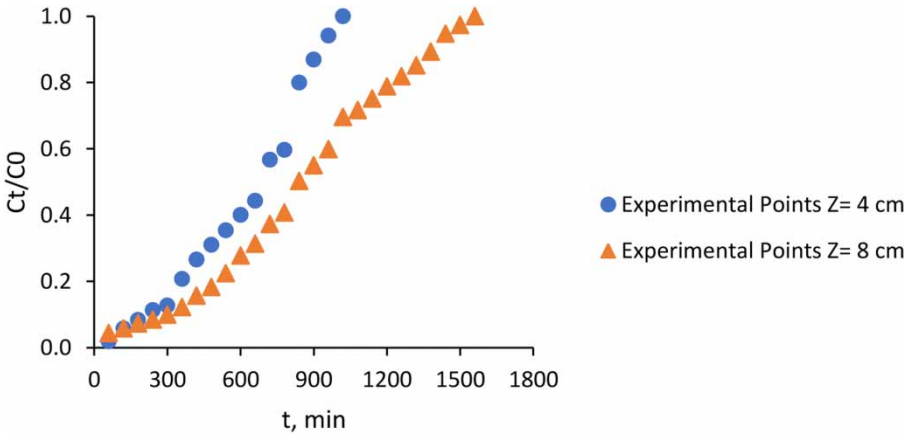

Figure 5 | WSA breakthrough curves at different bed depths (C_0 = 20 mg/l, Q = 40 ml/min).

Downloaded from http://iwaponline.com/wst/article-pdf/81/10/2109/716478/wst081102109.pdf
by guest

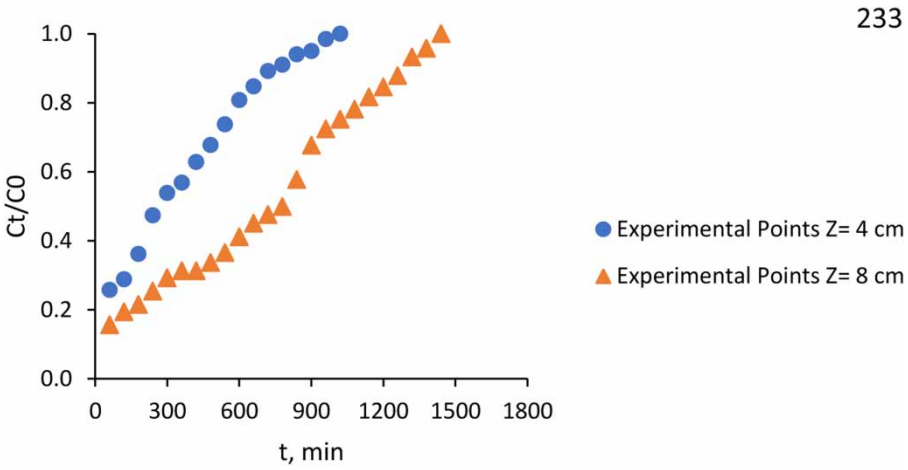

Figure 6 | CSA breakthrough curves at different bed depths ($C_0 = 20$ mg/l, Q = 40 ml/min).

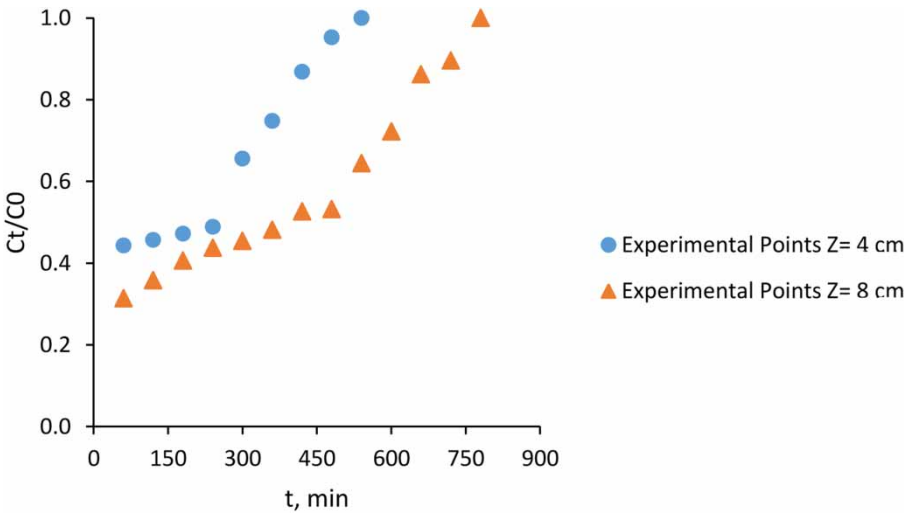

Figure 7 | WSA breakthrough curves at different bed depths ($C_0 = 60$ mg/l, Q = 40 ml/min).

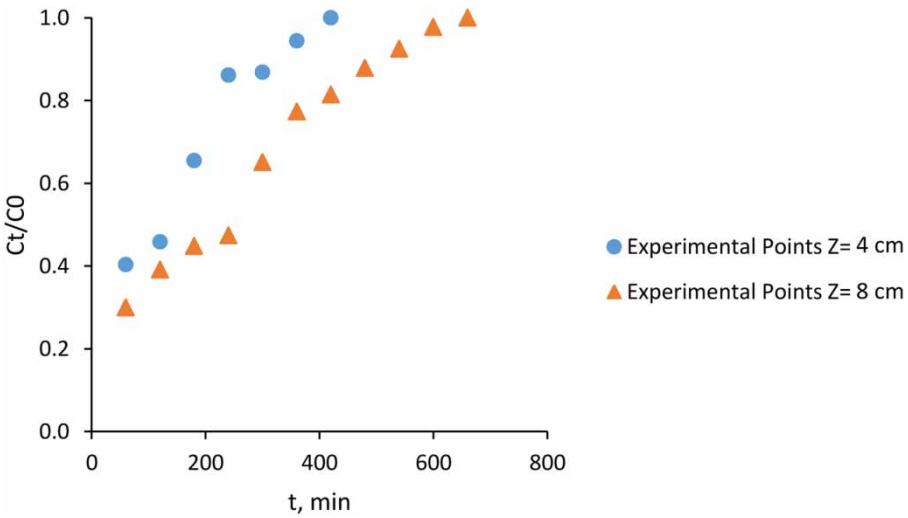

Figure 8 | CSA breakthrough curves at different bed depths ($C_0 = 60$ mg/l, Q = 40 ml/min).

Downloaded from http://iwaponline.com/wst/article-pdf/81/10/2109/716478/wst081102109.pdf
by guest

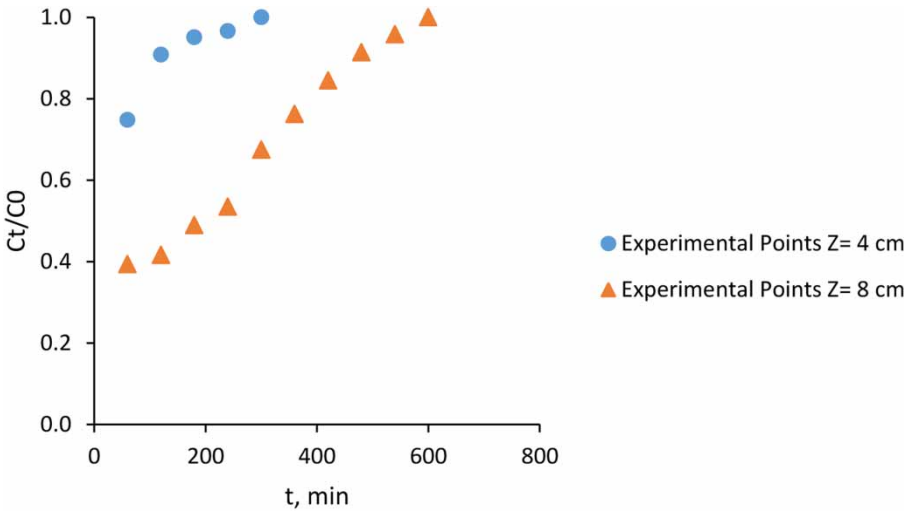

Figure 9 | WSA breakthrough curves at different bed depths ($C_0 = 100$ mg/l, Q = 40 ml/min).

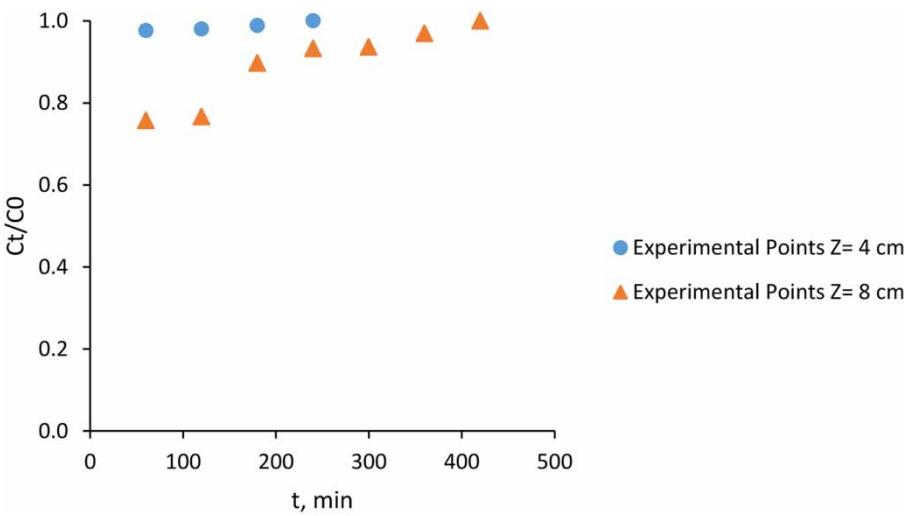

Figure 10 | CSA breakthrough curves at different bed depths ($C_0 = 100$ mg/l, Q = 40 ml/min).

time according to Equation (1) and that would be a great criterion for the performance of an adsorbent to treat more volumes of the influent. Also, with increase in the bed depth, the breakthrough curve slope decreases and as a result, there is a wide mass transfer zone. These observations, increasing the saturation time and removal efficiency by increasing the bed depth, are in complete agreement with the CAC results, which are shown in Figures 11–16. Another study was about removing phenol from aqueous solution using surfactant-modified alumina, and similar results were obtained by changing the bed depth (Adak & Pal 2006). In the study mentioned, the adsorbent bed depth of 10 cm was used to remove phenol with a concentration of 50 mg l^{-1} and the adsorbent was saturated in 300 minutes, but in the virtually similar experimental condition, when we investigated phenol removal with influent concentration of 60 mg l^{-1} by an adsorbent bed depth of 8 cm, the saturation occurred after 780 and 660 minutes for WSA and CSA, respectively. Adak and Pal (Adak & Pal 2006) concluded that saturation time decreases with increase in the flow rate. The comparison indicates that although the flow rate was 8.5 ml min^{-1} in their study, which was lower compared to flow rate of 40 ml min^{-1} in the current study, WSA and CSA have longer saturation time, which would be considered as their advantage to surfactant-modified alumina. On the other hand, surfactant-modified alumina was able to completely remove phenol (corresponding to $C_t/C_0 = 0$) until 180

Downloaded from http://iwaponline.com/wst/article-pdf/81/10/2109/716478/wst081102109.pdf
by guest

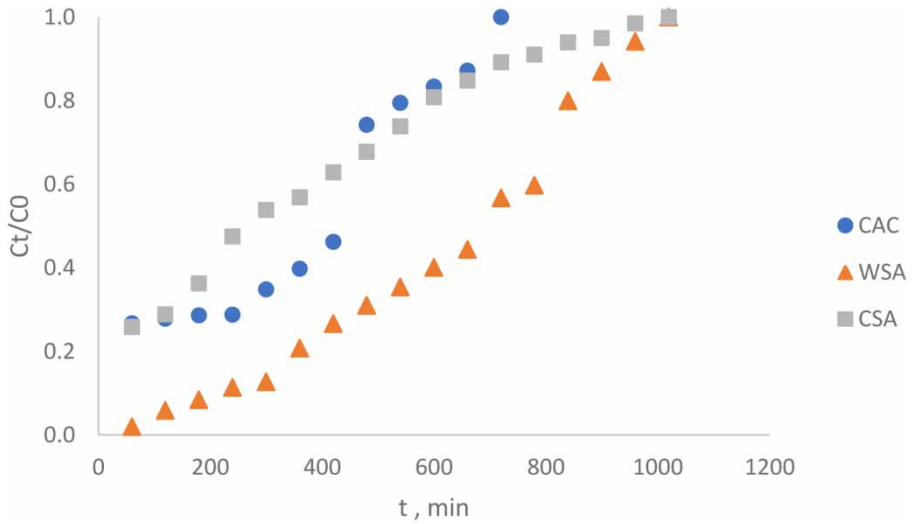

Figure 11 | Breakthrough curves at different adsorbent types ($C_0 = 20$ mg/l, Z = 4 cm, Q = 40 ml/min).

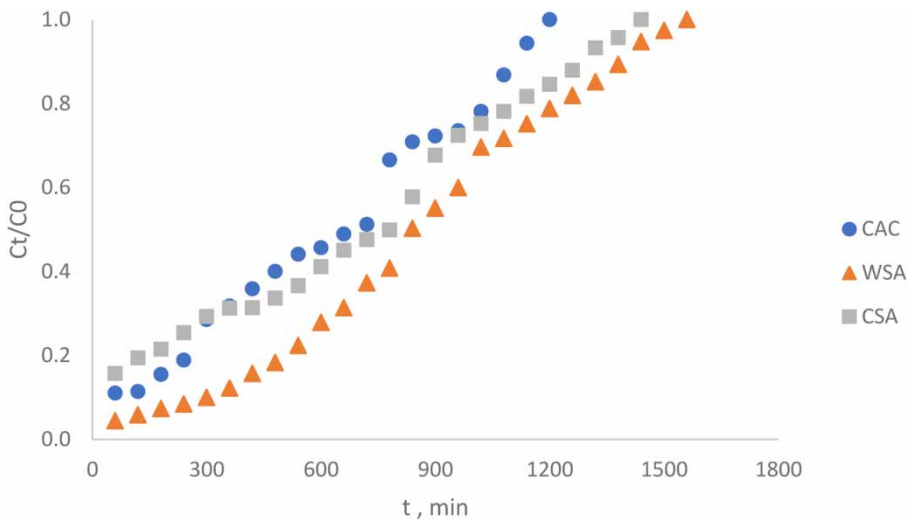

Figure 12 | Breakthrough curves at different adsorbent types ($C_0 = 20$ mg/l, Z = 8 cm, Q = 40 ml/min).

minutes after starting the experiment while the first values of C_t/C_0 in this study, which are measured after 60 minutes, are 0.712 and 0.721 for WSA and CSA, respectively, which states that unlike surfactant-modified alumina, WSA and CSA are not successful at full removal of phenol in this specific experimental condition.

Effect of type of adsorbent

The performance of adsorbents in a constant concentration of influent phenol, and also with the same bed depth of adsorbents, was evaluated. In this section, for comparing the performance of WSA and CSA, the results of CAC are also given. The breakthrough curves obtained by changing the adsorbent type are shown in Figures 11–16. As can be seen, among the three adsorbents, WSA has a better performance than the others, which is found both in the higher removal efficiency of phenol and in the longer saturation time, which results in more diffused breakthrough curves. For instance, in Figure 14, WSA is completely saturated after 780 minutes, while this time for CSA and CAC is 660 and 600 minutes, respectively. This finding is important when it is realized that WSA, which is produced from a cheap agricultural product, walnut shell, could be a better option to use as an adsorbent than CAC, which costs much more for the users. It also indicates that in

Downloaded from http://iwaponline.com/wst/article-pdf/81/10/2109/716478/wst081102109.pdf
by guest

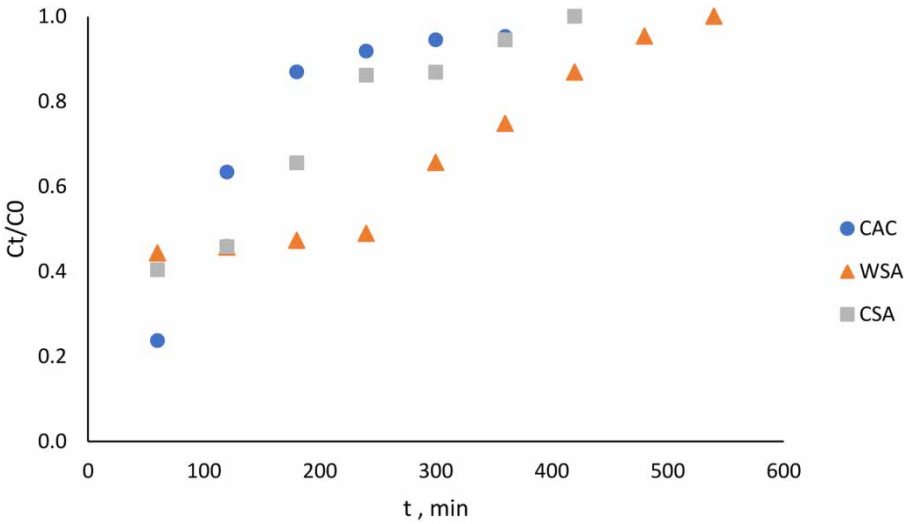

Figure 13 | Breakthrough curves at different adsorbent types ($C_0 = 60$ mg/l, Z = 4 cm, Q = 40 ml/min).

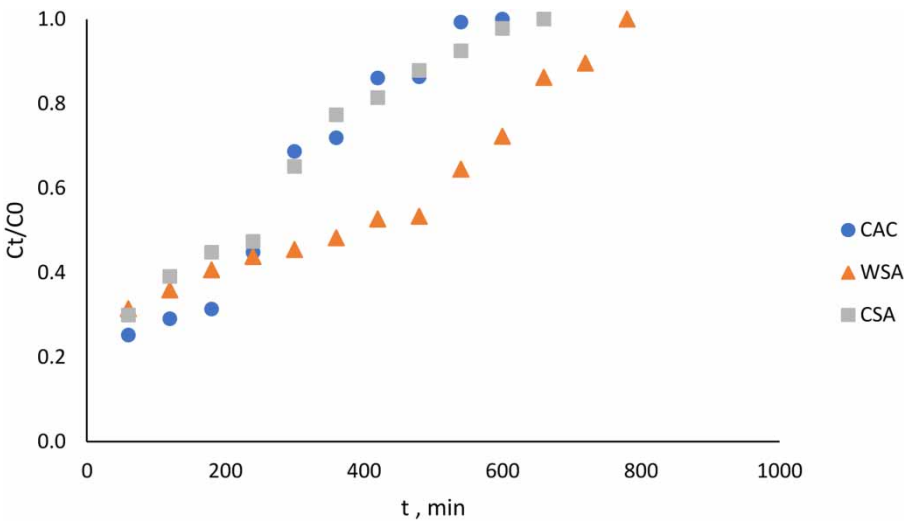

Figure 14 | Breakthrough curves at different adsorbent types ($C_0 = 60$ mg/l, Z = 8 cm, Q = 40 ml/min).

order to select the adsorbent, WSA should be considered of higher priority in comparison to CSA and CAC.

Effect of influent phenol concentration

Figures 17–20 show the breakthrough curves at different influent phenol concentrations. As expected, the reduction of the influent concentration results in a better and longer breakthrough curve. By increasing the concentration of phenol, the binding sites are saturated more quickly and the column then becomes saturated in less time. In lower phenol concentrations, breakthrough curves are more dispersed, but the higher the influent concentration, the steeper the breakthrough curve slope. As Equation (1) states, the treated volume is expected to be lowest at a phenol concentration of 100 mg l^{-1} since saturation happens earlier compared to the others. So, the results show that the change in the influent concentration has an effect on saturation time and speed. It can also be seen that at the same time for all of the adsorbents, the highest removal efficiency (the lowest value of C_t/C_0) occurs in 20 mg l^{-1} of phenol concentration which means that by increasing the phenol concentration, removal efficiency decreases. For example, according to Figure 17, 60 minutes after the start of the

Downloaded from http://iwaponline.com/wst/article-pdf/81/10/2109/716478/wst081102109.pdf
by guest

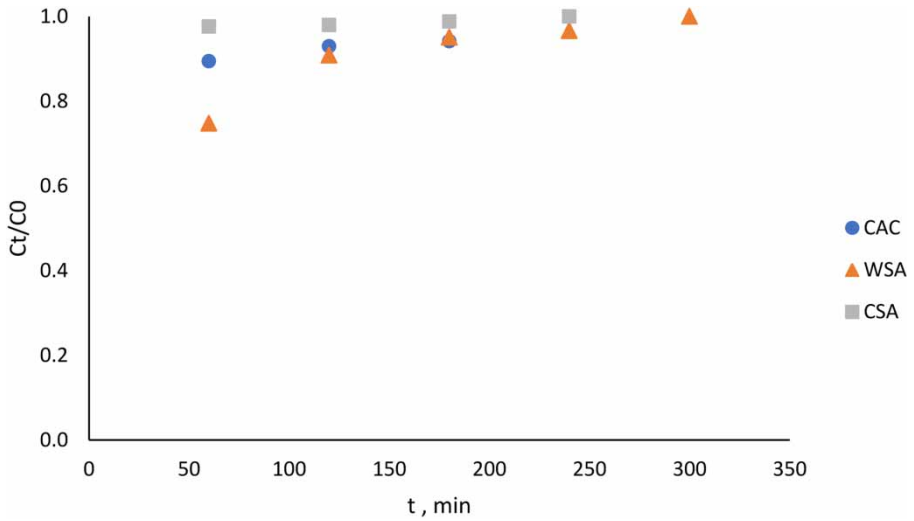

Figure 15 | Breakthrough curves for different adsorbent types ($C_0 = 100$ mg/l, Z = 4 cm, Q = 40 ml/min).

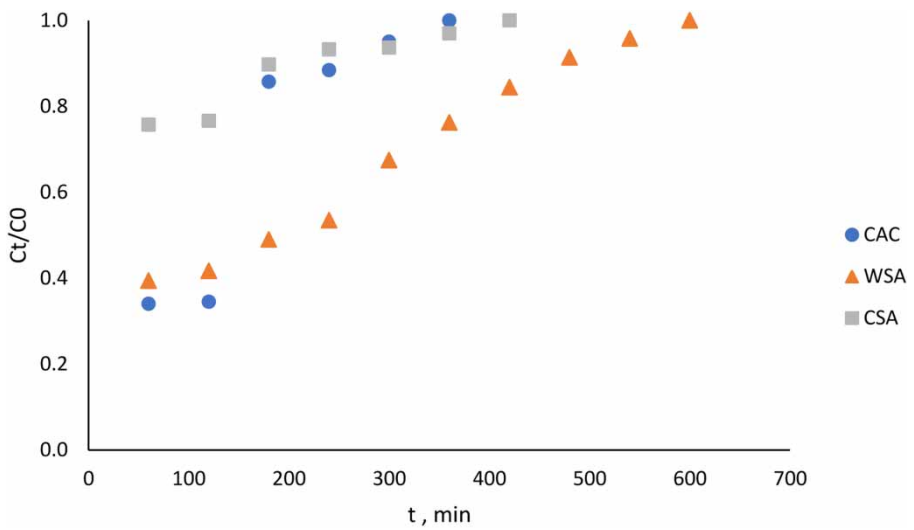

Figure 16 | Breakthrough curves for different adsorbent types ($C_0 = 100$ mg/l, Z = 8 cm, Q = 40 ml/min).

experiment, when the first samples are taken, the values of C_t/C_0 for 4 cm of WSA are 0.019, 0.443 and 0.748; in other words, removal efficiency is 98.1%, 55.7% and 25.2% for phenol concentrations of 20, 60 and 100 mg l^{-1}, respectively. Figure 19 shows that the same goes for 4 cm of CSA when at similar times, C_t/C_0 values are 0.258, 0.404 and 0.976 or removal efficiency is 74.2%, 59.6% and 2.4% for phenol concentrations of 20, 60 and 100 mg l^{-1}, respectively. This process continues throughout the experiment. Similar studies that aimed to investigate phenol removal by nutshell activated carbon (Goud *et al.* 2005), immobilized activated sludge (Aksu & Gönen 2004) and SDS-modified alumina (Adak & Pal 2006) confirms the results of this research obtained by phenol concentration change. If we compare our results to Aksu and Gonen's (Aksu & Gönen 2004), in the similar experimental condition when they used immobilized activated sludge with a bed depth of 6 cm and phenol concentration of 100 mg $l^{-1}$and we used adsorbent bed depth of 8 cm with the same influent concentration, the saturation time for sludge was almost 75 minutes, whereas WSA and CSA saturated after 600 and 420 minutes, respectively. It should be considered that in their study the flow rate was 0.8 ml min^{-1} compared to 40 ml min^{-1} in the present study, which by their findings

Downloaded from http://iwaponline.com/wst/article-pdf/81/10/2109/716478/wst081102109.pdf
by guest

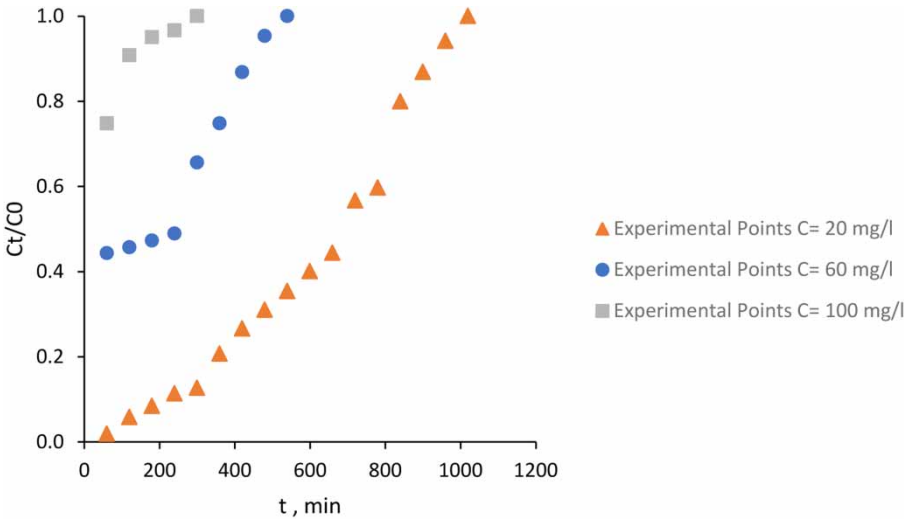

Figure 17 | WSA breakthrough curves at different influent phenol concentrations (Z = 4 cm).

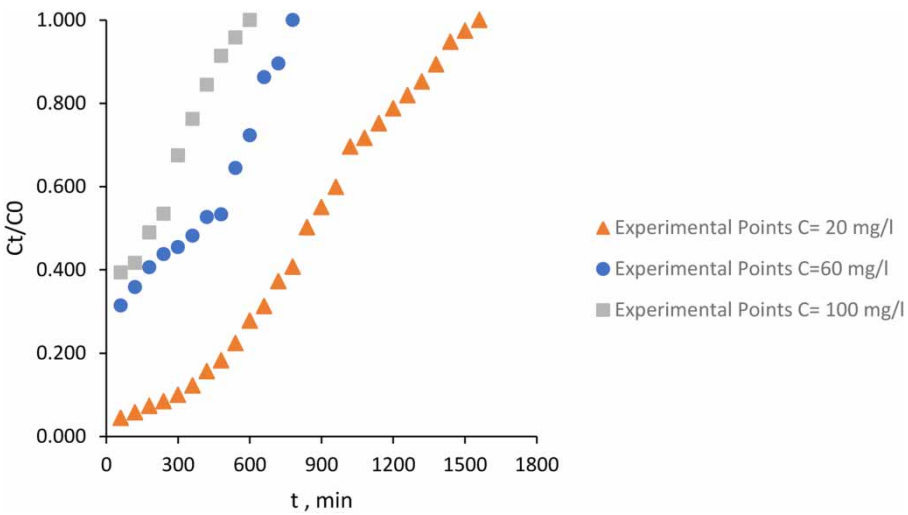

Figure 18 | WSA breakthrough curves at different influent phenol concentrations (Z = 8 cm).

saturation time is expected to rise with decreasing flow rate. This great difference in saturation time, despite the higher flow rate, indicates the advantage of WSA and CSA over immobilized activated sludge.

Thomas model

The Thomas model parameters were determined by fitting the column results with the model. To determine kinetic coefficients, linear regression was performed on each series of results. Studies indicate that for WSA, all of the regressed lines have an acceptable coefficient of determination ranging from 0.944 to 0.985, except for 60 mg l^{-1} of influent phenol concentration. In the case of CSA, the range is from 0.943 to 0.974, showing good performance of the model in fitting the experimental results. In addition, due to inadequate results of the experiment for 4 cm of CSA with phenol concentration of 100 mg l^{-1}, the model was not able to predict the breakthrough curve and the parameters were not determined. Tables 3 and 4 present the values of k_{Th} and q_0 for WSA and CSA, respectively. As is obvious in these tables, with increase in influent phenol concentration as well as increase in depth of the adsorbent bed, the values of k_{Th} decrease. Figures 21–24

Downloaded from http://iwaponline.com/wst/article-pdf/81/10/2109/716478/wst081102109.pdf
by guest

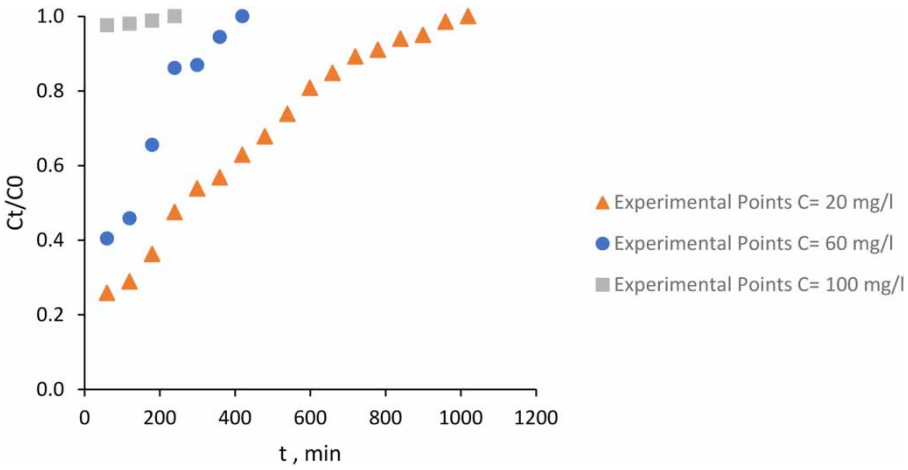

Figure 19 | CSA breakthrough curves at different influent phenol concentrations (Z = 4 cm).

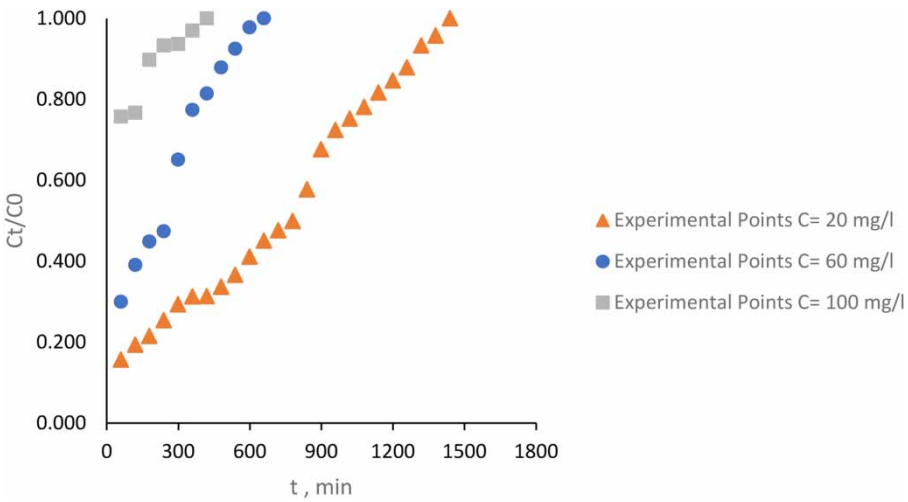

Figure 20 | CSA breakthrough curves at different influent phenol concentrations (Z = 8 cm).

Table 3 | Thomas model parameters for WSA

C_0 (mg l^{-1})	Q (ml min^{-1})	X (cm)	k_{Th} (ml min^{-1} mg^{-1})	q_0 (mg g^{-1})	R^2	$R^2_{adjusted}$
20	40	4	0.305	52.12	0.960	0.957
20	40	8	0.205	35.38	0.985	0.984
60	40	4	0.123	42.32	0.851	0.826
60	40	8	0.067	39.82	0.874	0.861
100	40	4	0.125	18.69	0.944	0.916
100	40	8	0.075	36.58	0.953	0.946

show the predicted breakthrough curves in different laboratory conditions using the Thomas model and it is clear that there is a good match between the results of the experiment and the predicted results of the Thomas model.

Downloaded from http://iwaponline.com/wst/article-pdf/81/10/2109/716478/wst081102109.pdf
by guest

Table 4 | Thomas model parameters for CSA

C_0(mg l^{-1})	Q (ml min^{-1})	X (cm)	k_{Th} (ml min^{-1} mg^{-1})	q_0 (mg g^{-1})	R^2	$R^2_{adjusted}$
20	40	4	0.260	23.65	0.974	0.972
20	40	8	0.160	25.99	0.958	0.956
60	40	4	0.187	26.57	0.961	0.951
60	40	8	0.133	24.42	0.957	0.952
100	40	4	–	–	–	–
100	40	8	0.079	14.07	0.943	0.929

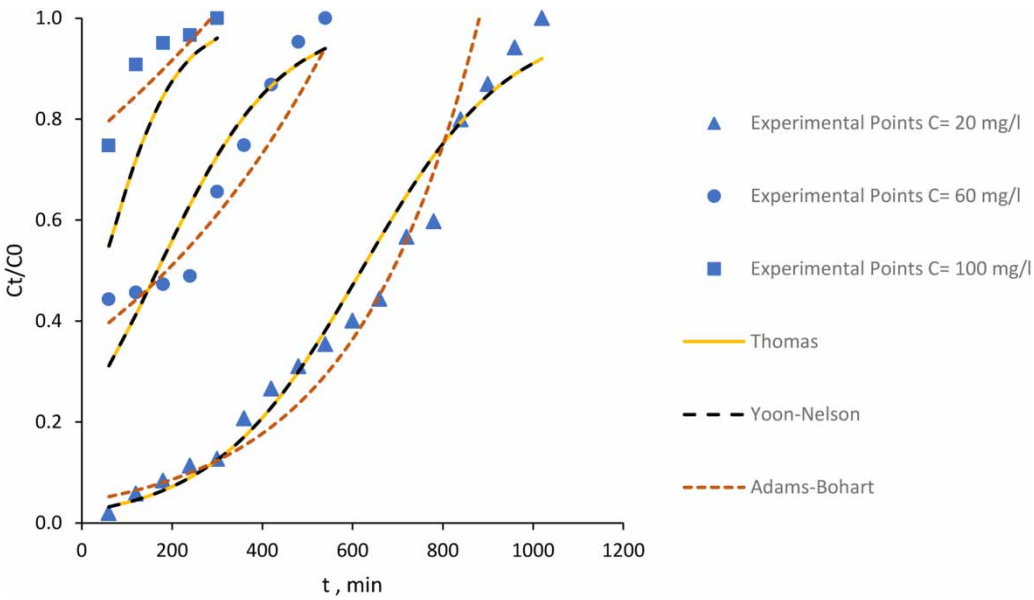

Figure 21 | WSA experimental and predicted breakthrough curves (Z = 4 cm).

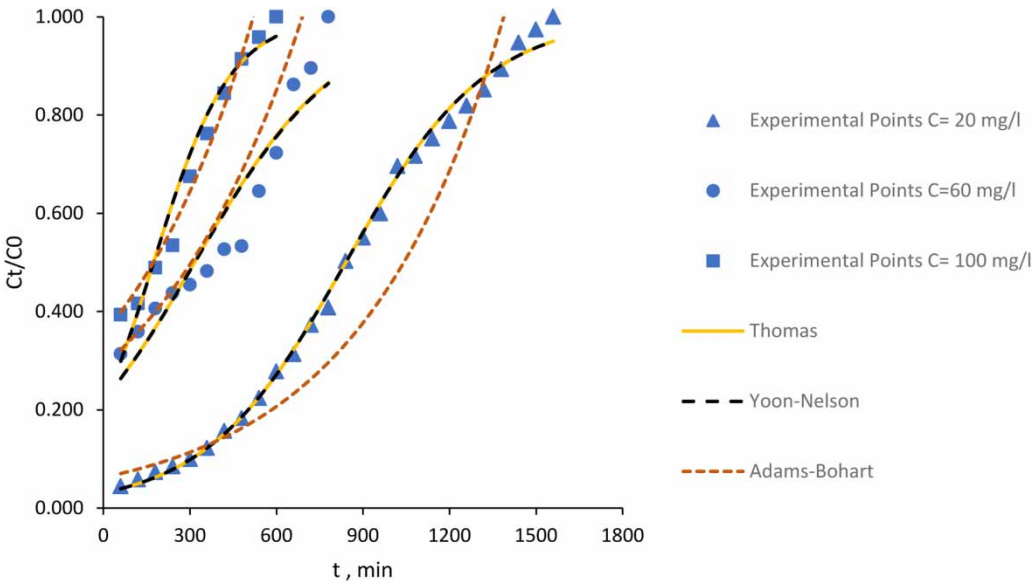

Figure 22 | WSA experimental and predicted breakthrough curves (Z = 8 cm).

Downloaded from http://iwaponline.com/wst/article-pdf/81/10/2109/716478/wst081102109.pdf
by guest

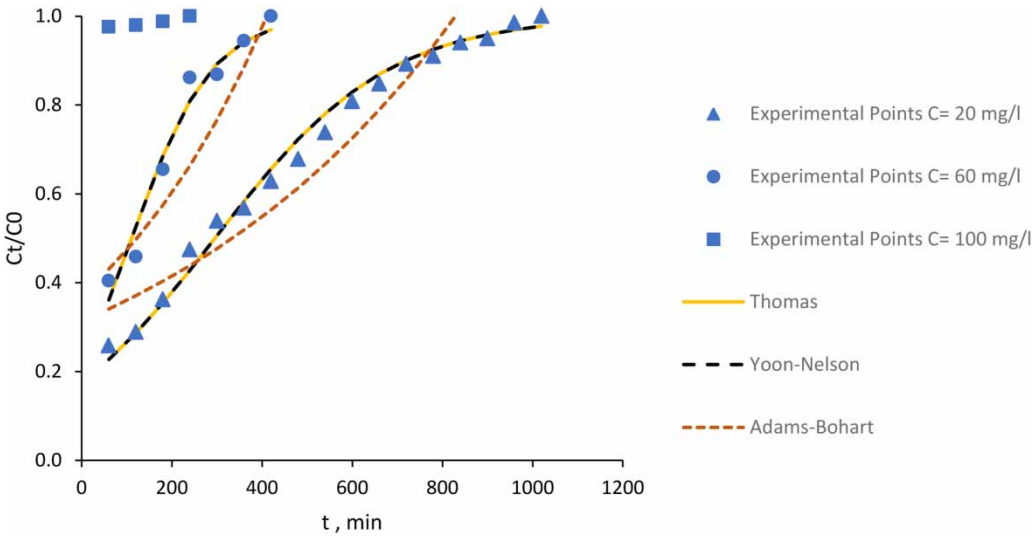

Figure 23 | CSA experimental and predicted breakthrough curves (Z = 4 cm).

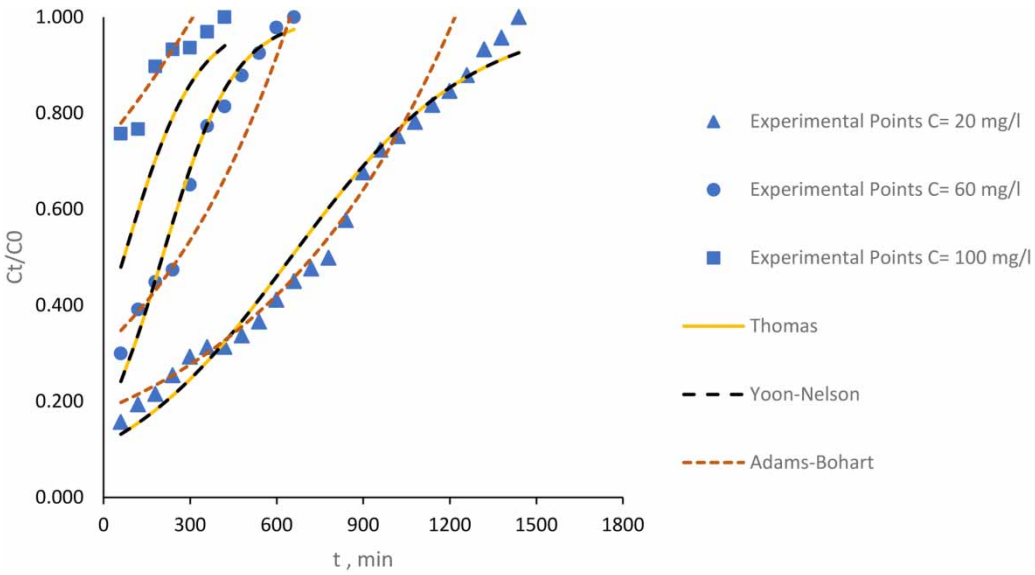

Figure 24 | CSA experimental and predicted breakthrough curves (Z = 8 cm).

Yoon-Nelson model

Tables 5 and 6 present the values of k_{YN} and τ for WSA and CSA, respectively. According to these tables, by increasing the influent phenol concentration, k_{YN} increases and τ decreases because the column saturation process is faster in those conditions. It is also observed that with increase in the bed depth, k_{YN} decreases and τ increases. These results are similar to the results of studies conducted by other researchers that used different adsorption systems (Aksu & Gönen 2004; Calero *et al.* 2009; Han *et al.* 2009).

Table 5 | Yoon-Nelson model parameters for WSA

C_0 (mg l^{-1})	Q (ml min^{-1})	X (cm)	k_{YN} (min^{-1})	τ (min)	R^2	$R^2_{adjusted}$
20	40	4	0.0061	618.9	0.960	0.957
20	40	8	0.0041	840.2	0.985	0.984
60	40	4	0.0074	167.1	0.851	0.826
60	40	8	0.0040	316.8	0.874	0.861
100	40	4	0.0125	44.4	0.944	0.916
100	40	8	0.0075	173.8	0.953	0.946

Downloaded from http://iwaponline.com/wst/article-pdf/81/10/2109/716478/wst081102109.pdf
by guest

Table 6 | Yoon-Nelson model parameters for CSA

C_0 (mg l^{-1})	Q (ml min^{-1})	X (cm)	k_{YN} (min^{-1})	τ (min)	R^2	$R^2_{adjusted}$
20	40	4	0.0052	295.6	0.974	0.972
20	40	8	0.0032	649.6	0.958	0.956
60	40	4	0.0112	110.9	0.961	0.951
60	40	8	0.0080	203	0.957	0.952
100	40	4	–	–	–	–
100	40	8	0.0079	70.3	0.943	0.929

Also, with bed depth increasing, k_{YN} values decrease and τ values increase, as can be seen from the tables. Figures 21–24 show the experimental and predicted breakthrough curves. The breakthrough curves obtained from the experiments are very close to the predicted breakthrough curves of the Yoon-Nelson model, which denotes that the model correlates well with the effects of the influent phenol concentration and the adsorbent bed depth. The high values of R^2 that are given in the tables confirm the observation.

Adams-Bohart model

The values of k_{AB} and N_0 for WSA and CSA are presented in Tables 7 and 8, respectively. As expected, in most conditions, N_0 decreases with decreasing bed depth and increases with increasing influent phenol concentration. On the other hand, the values of k_{AB} decrease when influent phenol concentration increases. These results are similar to the results of studies conducted by other researchers (Aksu & Gönen 2004; Calero et al. 2009; Han et al. 2009). The values of R^2 for WSA vary from 0.912 to 0.977. The exception is for the experiment of 4 cm of bed depth and 100 mg l^{-1} of phenol concentration. For CSA, R^2 values are slightly lower than WSA, which indicates that the model has better fitness to WSA experimental results compared to CSA results. Figures 21–24 show the predicted and experimental breakthrough curves. These figures illustrate that the Adams-Bohart model is suitable for prediction of the initial part of the breakthrough curve, because in high concentrations, more contradictions between the predicted and experimental breakthrough curves are observed in the column.

Table 7 | Adams-Bohart model parameters for WSA

C_0 (mg l^{-1})	Q (ml min^{-1})	X (cm)	k_{AB} (l min^{-1} mg^{-1})	N_0 (mg l^{-1})	R^2	$R^2_{adjusted}$
20	40	4	0.00018	33,158.1	0.912	0.906
20	40	8	0.00010	26,127.2	0.932	0.929
60	40	4	0.00003	64,751.8	0.946	0.938
60	40	8	0.00003	38,948.9	0.977	0.941
100	40	4	0.00001	54,027.8	0.781	0.708
100	40	8	0.00002	48,916.8	0.967	0.963

Table 8 | Adams-Bohart model parameters for CSA

C_0 (mg l^{-1})	Q (ml min^{-1})	X (cm)	k_{AB} (l min^{-1} mg^{-1})	N_0 (mg l^{-1})	R^2	$R^2_{adjusted}$
20	40	4	0.00007	31,217.2	0.884	0.876
20	40	8	0.00007	22,924.8	0.973	0.972
60	40	4	0.00004	46,427.2	0.892	0.870
60	40	8	0.00003	36,539.3	0.925	0.917
100	40	4	–	–	–	–
100	40	8	0.00001	29,112.9	0.873	0.848

Downloaded from http://iwaponline.com/wst/article-pdf/81/10/2109/716478/wst081102109.pdf
by guest

CONCLUSIONS

The adsorption of phenol from leachate on WSA, CSA and CAC was investigated in a continuous fixed-bed column. The effect of several parameters including adsorbent bed depth, influent phenol concentration and type of adsorbent on adsorption was studied. Three models of Yoon-Nelson, Adams-Bohart and Thomas were applied to predict the performance of the adsorbents and describe the breakthrough curve. Also, to investigate the effect of phenol on the chemical mechanism of adsorbents through adsorption, FTIR spectroscopy was used. Based on the results of experiments, the following conclusions can be made:

- The chemical mechanism and the hydrogen bond between hydrogen of the functional groups and the hydrogen of the phenol hydroxyl group are effective in the phenol adsorption.
- By increasing the bed depth of adsorbent in the column, phenol removal efficiency and saturation time increases significantly. Also, with increase in the bed depth, the breakthrough slope curve decreases.
- By increasing the influent concentration, saturation time of the column decreases. Also, at lower concentrations of the phenol, breakthrough curves are more dispersed, but the higher the influent concentration, so the breakthrough curve slope increases.
- Among the selected adsorbents, WSA is the best option for use as an adsorbent to remove phenol from the leachate due to the higher removal efficiency of phenol and longer saturation time.
- The optimum removal efficiency of adsorbents occurs when phenol concentration is lowest and the bed depth of the adsorbents is highest.
- There is a good match between the results of the experiment and the predicted results of the models.

REFERENCES

Adak, A. & Pal, A. 2006 Removal of phenol from aquatic environment by SDS-modified alumina: batch and fixed bed studies. *Sep. Purif. Technol.* **50** (2), 256–262.

Aizpuru, A., Malhautier, L., Roux, J. C. & Fanlo, J. L. 2003 Biofiltration of a mixture of volatile organic compounds on granular activated carbon. *Biotechnol. Bioeng.* **83** (4), 479–488.

Aksu, Z. & Gönen, F. 2004 Biosorption of phenol by immobilized activated sludge in a continuous packed bed: prediction of breakthrough curves. *Process Biochem.* **39** (5), 599–613.

Aksu, Z. & Yener, J. 2001 A comparative adsorption/biosorption study of mono-chlorinated phenols onto various sorbents. *Waste Manag.* **21** (8), 695–702.

Aziz, S. Q., Aziz, H. A., Yusoff, M. S. & Mohajeri, S. 2012 Removal of phenols and other pollutants from different landfill leachates using powdered activated carbon supplemented SBR technology. *Env. Monit Assess* **184** (10), 6147–6158.

Bagreev, A., Rahman, H. & Bandosz, T. J. 2001 Thermal regeneration of a spent activated carbon previously used as hydrogen sulfide adsorbent. *Carbon N. Y.* **39** (9), 1319–1326.

Calero, M., Hernáinz, F., Blázquez, G., Tenorio, G. & Martín-Lara, M. A. 2009 Study of Cr (III) biosorption in a fixed-bed column. *J. Hazard. Mater.* **171** (1–3), 886–893.

Dan, A., Fujii, D., Soda, S., Machimura, T. & Ike, M. 2017 Removal of phenol, bisphenol A, and 4-tert-butylphenol from synthetic landfill leachate by vertical flow constructed wetlands. *Sci. Total Environ.* **578**, 566–576.

Goud, V. V., Rao, M. S., Mohanty, K. & Jayakumar, N. S. 2005 Phenol removal from aqueous solutions by tamarind nutshell activated carbon: batch and column studies. *Chem. Eng. Technol.* **28** (7), 814–821.

Gupta, V. K., Sharma, S., Yadav, I. S. & Mohan, D. 1998 Utilization of bagasse fly ash generated in the sugar industry for the removal and recovery of phenol and p-nitrophenol from wastewater. *J. Chem. Technol. Biotechnol.* **71** (2), 180–186.

Han, R., Wang, Y., Zhao, X., Wang, Y., Xie, F., Cheng, J. & Tang, M. 2009 Adsorption of methylene blue by phoenix tree leaf powder in a fixed-bed column : experiments and prediction of breakthrough curves fixed-bed column: experiments and prediction. *Desalination* **245** (1–3), 284–297.

Lim, J. L. & Okada, M. 2005 Regeneration of granular activated carbon using ultrasound. *Ultrason. Sonochem.* **12** (4), 277–282.

Mahvi, A., Maleki, A. & Eslami, A. 2004 Potential of rice husk and rice husk ash for phenol removal in aqueous systems. *Am. J. Appl. Sci.* **4** (1), 321–326.

Martin, R. J. & Ng, W. J. 1987 The chemical regeneration and subsequent volatilization of exhausted activated carbon. *Water Res.* **21** (8), 961–965.

Mohammadi, S., Kargari, A., Sanaeepur, H., Abbassian, K., Najafi, A. & Mofarrah, E. 2015 Phenol removal from industrial wastewaters: a short review. *Desalin. Water Treat.* **53** (8), 2215–2234.

Narbaitz, R. M. & Karimi-Jashni, A. 2009 Electrochemical regeneration of granular activated carbons loaded with phenol and natural organic matter. *Environ. Technol.* **30** (1), 27–36.

Orupold, K., Tenno, T. & Henrysson, T. 2000 Biological lagooning of phenols-containing oil shale ash heaps leachate. *Water Res.* **34** (18), 4389–4396.

Pajooheshfar, S. P. & Saeedi, M. 2009 Adsorptive removal of phenol from contaminated water and wastewater by activated carbon, almond, and walnut shells charcoal. *Water Environ. Res.* **81** (6), 641–648.

Rao, J. R. & Viraraghavan, T. 2002 Biosorption of phenol from an aqueous solution by aspergillus Niger biomass. *Bioresour. Technol.* **85** (2), 165–171.

Downloaded from http://iwaponline.com/wst/article-pdf/81/10/2109/716478/wst081102109.pdf
by guest

Rengaraj, S., Moon, S. & Sivabalan, R. 2002 Agricultural solid waste for the removal of organics: adsorption of phenol from water and wastewater by palm seed coat activated carbon. *Waste Manag.* **22** (5), 543–548.

Rodríguez, J., Castrillón, L., Marañón, E., Sastre, H. & Fernández, E. 2004 Removal of non-biodegradable organic matter from landfill leachates by adsorption. *Water Res.* **38** (14–15), 3297–3303.

Sanjay, M., Amit, D. & Mukherjee, S. N. 2013 Applications of adsorption process for treatment of landfill leachate. *J. Environ. Dev.* **8** (2), 365–370.

Shende, R. V. & Mahajani, V. V. 2002 Wet oxidative regeneration of activated carbon loaded with reactive dye. *Waste Manag.* **22** (1), 73–83.

Show, P. L., Pal, P., Leong, H. Y., Juan, J. C. & Ling, T. C. 2019 A review on the advanced leachate treatment technologies and their performance comparison: an opportunity to keep the environment safe. *Environ. Monit. Assess.* **191** (227), 1–28.

Simaratanamongkol, A. & Thiravetyan, P. 2010 Decolorization of melanoidin by activated carbon obtained from bagasse bottom ash. *J. Food Eng.* **96** (1), 14–17.

Srivastava, S. K., Gupta, V. K., Johri, N. & Mohan, D. 1995 Removal of 2,4,6-trinitrophenol using bagasse fly ash – a sugar industry waste material. *Indian J. Chem. Technol.* **2**, 333–336.

Srivastava, S. K., Tyagi, R., Pal, N. & Mohan, D. 1997 Process development for removal of substituted phenol by carbonaceous adsorbent obtained from fertilizer waste. *J. Environ. Eng.* **123** (9), 842–851.

Srivastava, V. C., Swamy, M. M., Mall, I. D., Prasad, B. & Mishra, I. M. 2006 Adsorptive removal of phenol by bagasse fly ash and activated carbon: equilibrium, kinetics and thermodynamics. *Colloids Surfaces A* **272** (1–2), 89–104.

Streat, M., Patrick, J. W. & Perez, M. J. C. 1995 Sorption of phenol and para-chlorophenol from water using conventional and novel activated carbons. *Water Res.* **29** (2), 467–472.

Tsai, W. 1999 Adsorption properties and breakthrough model of 1, 1-dichloro-1-fluoroethane on activated carbons. *J. Hazard. Mater.* **69** (1), 53–66.

Volesky, B. 2003 *Sorption and Biosorption*. BV Sorbex, Montreal, Quebec, Canada.

Warah, R. 2001 UrbanWaste. In: *State of The World's Cities*, United Nations Centre for Human Settlements (Habitat), Nairobi, Kenya, pp. 70–71.

Wenzel, A., Gahr, A. & Niessner, R. 1999 TOC-removal and degradation of pollutants in leachate using a thin-film photoreactor. *Water Res.* **33** (4), 937–946.

Yakout, S. M. & Sharaf El-Deen, G. 2016 Characterization of activated carbon prepared by phosphoric acid activation of olive stones. *Arab. J. Chem.* **9** (2), 1155–1162. doi: 10.1016/j.arabjc.2011.12.002.

First received 16 January 2020; accepted in revised form 26 May 2020. Available online 9 June 2020

Downloaded from http://iwaponline.com/wst/article-pdf/81/10/2109/716478/wst081102109.pdf
by guest